Available online at www.sciencedirect.com

ScienceDirect

Procedia Engineering 132 (2015) 290 – 297

Procedia Engineering

www.elsevier.com/locate/procedia

The Manufacturing Engineering Society International Conference, MESIC 2015

On the study of the single-stage hole-flanging process by SPIF

M. Borrego[a], D. Morales-Palma[a,]*, A. J. Martínez-Donaire[a], G. Centeno[a], C. Vallellano[a]

[a]*Dpt. Mechanical and Manufacturing Engineering, University of Seville, Av. de los Descubrimientos s/n, 41092 Sevilla, Spain*

Abstract

Recent studies show the capability of single-point incremental forming to perform successfully hole-flanging operations using multi-stage strategies. The aim of this work is to investigate the ability of the SPIF process to perform hole-flanges in a single stage, contributing to a better understanding of the formability of the sheet in this demanding situation. To this end, a series of experimental tests in AA7075-O metal sheets are performed in order to evaluate the limiting forming ratio. The physical mechanisms controlling sheet failure during the process are analyzed and discussed. In the test conditions studied this failure is postponed necking followed by ductile fracture in the wall of the flange.

Peer-review under responsibility of the Scientific Committee of MESIC 2015

Keywords: Hole-flanging; Incremental sheet forming; Single-point incremental forming; Formability

1. Introduction

Conventional hole-flanging is a forming process used to manufacture circular or asymmetric flanges. In this process, a holed sheet, rigidly fix to a die with a blank holder, is plastically deformed mainly by bending and circumferential stretching with a punch. In hole-flanging by single-point incremental forming (SPIF), a flat sheet with a pre-cut hole is formed by a single-point rotating tool that progressively produces a smooth, round flanged lip. The forming tool is driven by a CNC machine following progressively a pre-established trajectory. The material is now mainly deformed by a combination of circumferential and radial stretching and bending. There are many industrial applications of this process such as strengthening the edge of the holes, improving its appearance or providing additional support for joining sheet parts to tubes, among others.

* Corresponding author. Tel.: +34 954 481355; fax: +34 954 460475.
E-mail address: dmpalma@us.es

Peer-review under responsibility of the Scientific Committee of MESIC 2015
doi:10.1016/j.proeng.2015.12.497

The formability of circular hole-flanging is traditionally characterized by the limiting forming ratio:

$$LFR = \frac{d_{\max}}{d_0} \tag{1}$$

i.e. the ratio of the maximum inside diameter dmax of the finished flange to the initial diameter d0 of the hole. The value of LFR depends on the mechanical properties of the material, surface quality of the initial hole edge, geometry of the forming punch, clearance between the punch and die and lubrication conditions, as it is pointed out in [1-4].

In general, high ductility materials formed by conventional sheet metal forming processes usually start failing by the onset of a localized necking. The material within this neck follows an instable deformation process, following approximately a near plane strain state, until the ductile fracture takes place. However, in SPIF (or any other incremental forming process), under a certain range of process parameters, the material may suffer a stable straining promoted by the delay or even complete inhibition of necking process, leading directly to the ductile fracture [5]. This failure mode is referred to as fracture after a postponed necking [2,5]. Both types of failure are commonly analyzed within the principal strain space by the well- known forming limit diagrams (FLD), which combines locus of the strains at onset of local necking (FLC, forming limit curve), and at the beginning of ductile fracture (FFL, fracture forming limit).

Recent studies show the capability of SPIF to perform successfully flanges using multi-stage strategies [1-4]. Despite of their inherent advantages in terms of simplicity, flexibility and sustainability, they have a great deficit in terms of time consuming. In this regards, there have been some attempts to reduce production time by performing hole-flanging processes by high-speed SPIF [6]. Nevertheless, the current state-of the art does not report a systematic study about the capability of performing flanges by SPIF in a single stage, what would meet the requirements previously claimed in a number of industrial situations. The aim of the present work is to contribute to understand the formability of the sheet in this demanding situation. Two important points need to be discussed, these are, the maximum flange that can be successfully formed by SPIF in a single stage, and the physical mechanisms controlling the sheet failure during this process. To this end, a series of experimental tests in AA7075-O metal sheets have been performed and analyzed.

2. Experimental procedure

Two series of experimental tests are being performed. The material tested is 7075-O aluminum alloy sheet of 1.6 mm thickness. Firstly, Nakazima tests are used to characterize the conventional forming limits of the material. Then, a series of single-stage hole flanging tests by SPIF are carried out.

2.1. Conventional forming limits

The material characterization of the AA7075-O sheets of 1.6 mm thickness was carried out by means of a series of Nakazima tests with a hemispherical punch of 100 mm diameter. The tests were performed in a universal sheet metal testing machine Erichsen 142-20 (see Fig. 1(a)) under the testing conditions of the standard ISO 12004-2:2008. The punch velocity was set to 1 mm/s and the lubricant at the interface punch-sheet was vaseline + PTFE sheet (0.05 mm thickness) + vaseline + PTFE sheet + vaseline. The tested specimens were continuously recorded up to failure by means of CCD cameras (Fig. 1(a)). Four different specimen geometries were tested to evaluate the sheet failure at different strain paths (uniaxial strain, near plane strain, biaxial strain and equibiaxial strain), as shown in Fig. 1(b).

The conventional FLD for the selected material was experimentally obtained and is depicted in Fig. 2. The strain history at the outer surface of the samples was evaluated via DIC (digital image correlation) using the 3D optical deformation measurement system ARAMIS®. The forming limit curve (FLC) was built following the recommendations given in the ISO 12004-2:2008. A time-dependent methodology proposed by the authors [7] was applied for detecting the onset of localized necking.

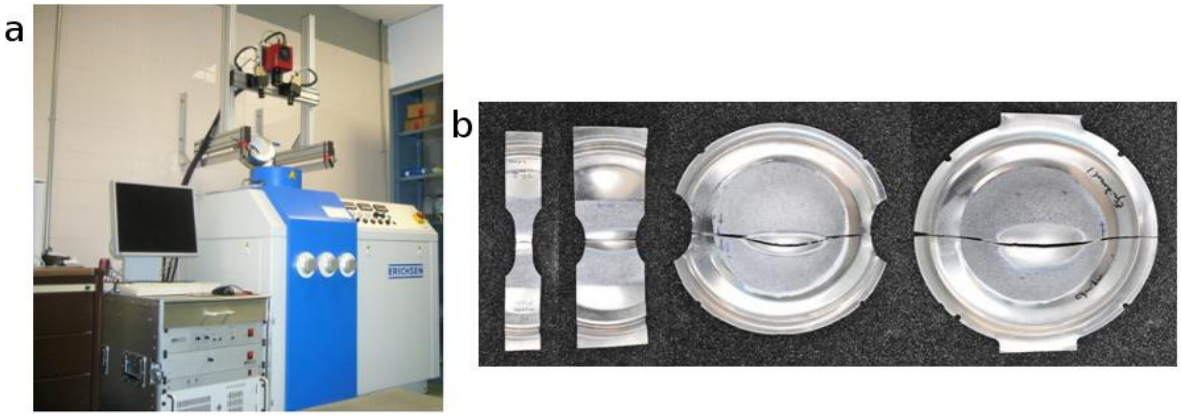

Fig. 1. (a) universal sheet metal testing machine and image recording system; (b) specimen geometries after testing.

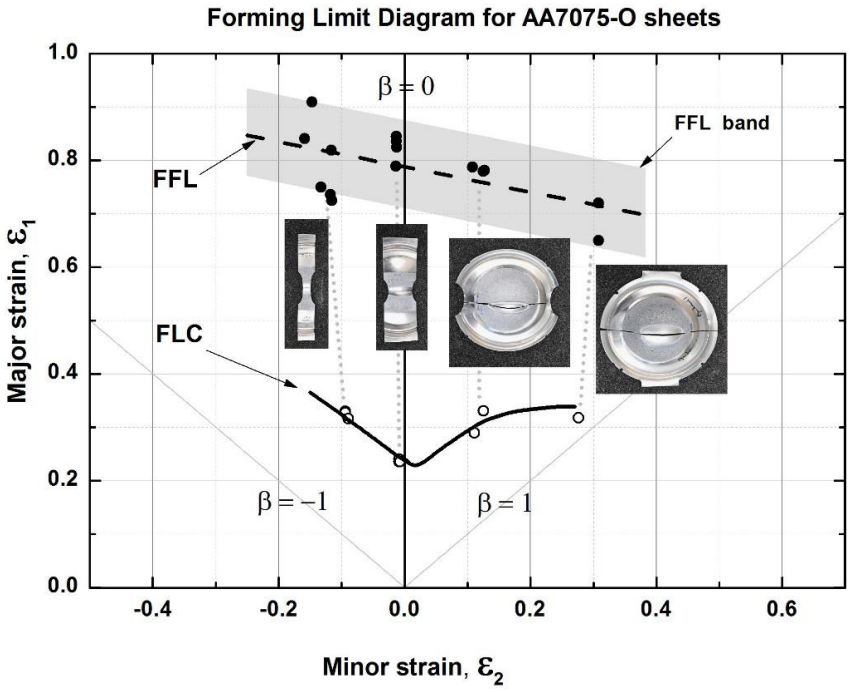

Fig. 2. Forming limit diagram (FLD) based on conventional Nakazima tests containing the forming limit curve (FLC) and the fracture forming line (FFL) for AA7075-O sheets of 1.6 mm thickness.

The forming fracture limit (FFL) was determined by a similar methodology as the one presented in [8]. The procedure starts by measuring at microscope the sheet thickness at the fracture point at both sides of the crack for every tested specimen. In addition, some tested specimens were cut perpendicularly to the crack initiation point to measure the thickness from a profile view and to validate the previous measurements along the crack. The thickness strain at fracture is then calculated (ε3f). The minor principal strain in the sheet plane (ε2f) was evaluated as the average value of the minor principal strain along the fracture line measured by ARAMIS® at the last image

recorded just before the crack appearance. The major principal strain (ε1f) was then calculated by volume conservation. The FFL scatter band of 10% represented in Fig. 2 agrees fairly well with the experimental scatter observed by Liu et al. [9] for the same material.

2.2. Single-stage hole-flanging tests

The single-stage hole-flanging tests were carried out on a 3-axis milling CNC machine. The experimental setup shown in Fig. 3(a) were used. Briefly, the SPIF setup is a blank holder and a backing plate with a 100 mm diameter hole, both fixed to the machine table through a rigid rig. A 20 mm diameter hemispherical punch is used as forming tool (see Fig. 3(b)).

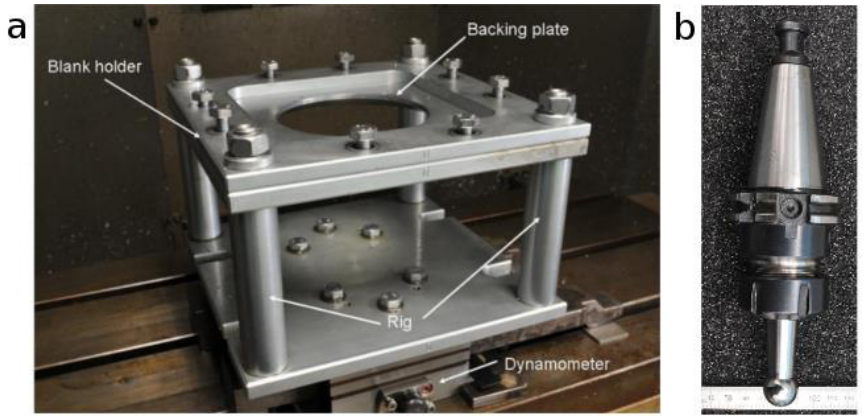

Fig. 3. (a) experimental setup for SPIF; (b) forming tool.

Fig. 4 shows a schema of the single-stage hole-flanging test. The tests try to achieve the final theoretical geometry of the hole in a single pass of the forming tool. In this case, a final hole of inner diameter d = 95.8 mm is programmed. Two different initials pre-cut holes were tested, d_0 = 56 and 58 mm. The forming trajectories were modelled and simulated in CATIA V5, using the machining workbench. The virtual model was used to optimize the tool trajectories according with the desired final geometry of the sheet.

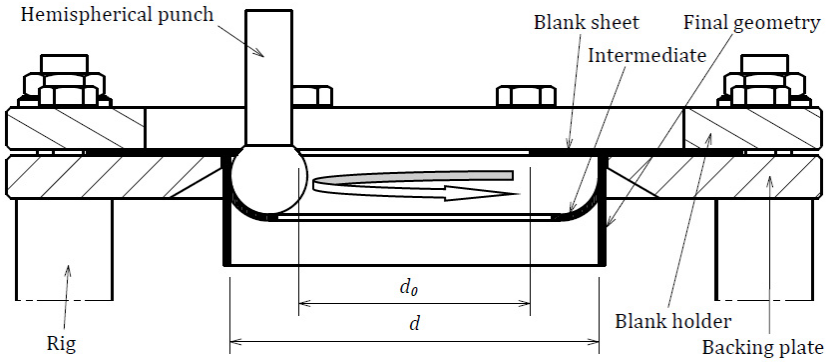

Fig. 4. Schema of the single-stage hole flanging process by SPIF.

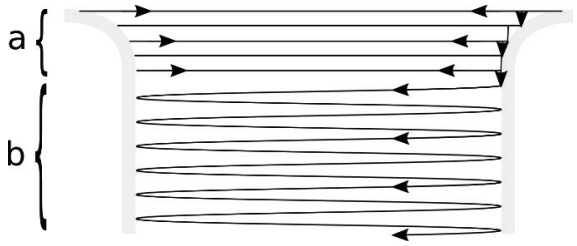

Fig. 5. Schema of the tool path: (a) z-level trajectory for the conical frustum; (b) cylindrical helical path.

The tool trajectory utilized to perform the hole flanging tests was divided in two steps. An initial z-level path following a conical frustum with varying slope in order to smoothly adjust the sheet to backing plate (see Fig. 5(a)). This is followed by a cylindrical helical path up to form the entire flange (see Fig. 5(b)). The helix is obtained by successive linear interpolations as allowed by the CNC control resolution. A step down of 0.2 mm/turn is used in both steps.

The rotation of the tool was locked and its feed rate was set to 1000 mm/min. Special lubricant Castrol Iloform TDN81 for metal forming applications was applied between the forming tool and the sheet blank. A Kistler® dynamometer was mounted between the machine-table and the SPIF frame (see Fig. 3(a)) in order to measure the forming forces in X, Y and Z axes during the tests. The forces were acquired using a home-made program using the commercial software LabVIEW.

To study the deformation and failure mechanisms, the strains in the sheet surface were obtained using circle grid analysis. Specimens were previously electro etched with a dot grid of with 1 mm initial diameter and spaced by 2 mm. The optical 3D forming analysis system ARGUS® was used to automatically compute the principal strains in the sheet.

3. Results and discussion

Fig. 6 shows the final configuration achieved by two specimens with pre-cut hole formed by SPIF using a 20 mm diameter tool. The deformation process was aborted just when the material failure was detected. As can be seen, this happened for the pre-cut hole of 56 mm diameter. Instead, no failure was detected for the specimen with a pre-cut hole of 58 mm, giving rise to a successful hole flanging operation by SPIF.

Table 1 shows the values of the hole expansion ratio (*HER*) theoretical and measured. In case of circular hole-flanges, the *HER* is defined as the ratio of the inside diameter d of the finished flange to the initial diameter d_0 of the hole:

$$HER = \frac{d}{d_0} \tag{2}$$

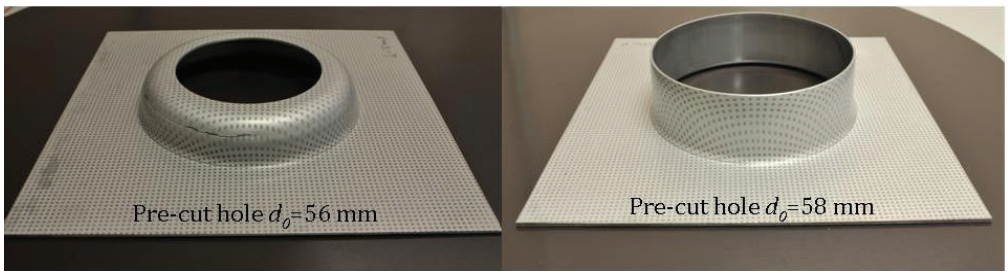

Fig. 6. Results of single-stage hole flanging tests by SPIF.

Table 1. Results of single-stage hole flanging tests.

d_0 (mm)	d_{th} (mm) (theory)	d (mm) (measured)	$HER = d_{th} / d_0$ (theory)	$HER = d / d_0$ (measured)	Result
56	95.8	–	1.71	–	Failure
58	95.8	93.7	1.65	1.62	Success

Note that the value of manufactured inside diameter d of the hole-flange and the HER measured is slightly minor than the theoretical design value. As can be seen, the *HER* measured is around 1.62. This means that the limiting forming ratio (*LFR*) of the sheet, i.e. maximum *HER*, is at least 1.62 ($LFR \geqslant 1.62$). This value agrees very well with the value expected in SPIF and for aluminum alloys [1,2]. The length of the flange was 27 mm for the specimen with the pre-cut hole of 58 mm diameter.

Fig. 7 shows a forming limit diagram with the experimental results of d_0 = 56 mm diameter hole. The *a-b-c-d-e* line in FLD represents the major and minor principal strains measured with ARGUS® along a straight line in the sheet surface (see dot-dashed line in the up-left image in Fig. 7). Note that point a is located near the non-deformed zone of the specimen, point *c* is right next to the crack, and point *e* is almost at the inner edge of the hole. The diamond-shaped point corresponds to the fracture strain measured at the crack lips following the procedure described in the previous section. As can be seen, the fracture point is slightly above the FFL scatter band obtained with Nakazima tests. This slight enhancement of formability at fracture in SPIF, regarding the Nakazima tests, is sometime attributed, among other factors, to the local and incremental character of the deformation and the bending effect inherent to the incremental forming process.

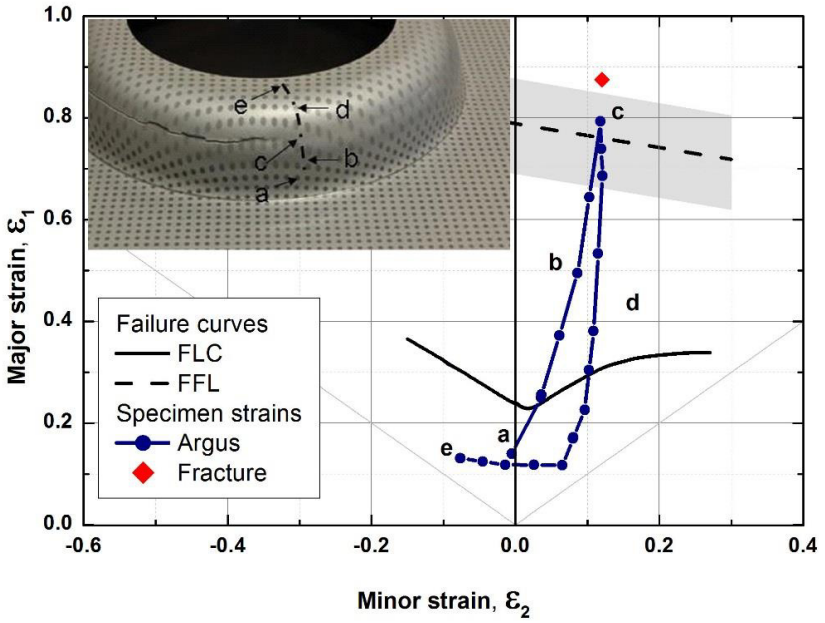

Fig. 7. Evolution of principal strains in the FLD for d_0 = 56 mm pre-cut hole specimen.

As can be seen in Fig. 7, the strains measured along the *a-b-c-d-e* line on the sheet surface exhibit two main trends on the FLD. The former (*a-b-c*) presents a quite vertical strain path towards biaxial conditions. Here the material is subjected to a combination of stretching and bending. This strain path is typical in multiple stage incremental forming [2,4]. The latter (*d-e*) is a path going from biaxial conditions near the crack to uniaxial

conditions at the edge of the hole, where the material is mainly circumferentially stretched. Note that in this case the small deformation of the material in the zone *d-e* is a consequence of the detention of the test.

Fig. 8 shows in detail the sheet failure zone for the d_0 = 56 mm pre-cut hole specimen. A through-thickness crack is clearly observed in the magnified fractography. A very incipient neck can be seen at the fracture zone, meaning that necking process was not able to fully develop before fracture appears. This fact is consistent with the pattern observed in the FLD, which reflect an evolution of the strains in the sheet well above the FLC and almost reaching the FFL in the neighborhood of the fracture zone. Therefore, the failure mode in this test is assumed to be a ductile fracture in mode I after a postponed necking process. The same phenomena has been observed in other studies in some aluminum alloys deformed by SPIF [2,10].

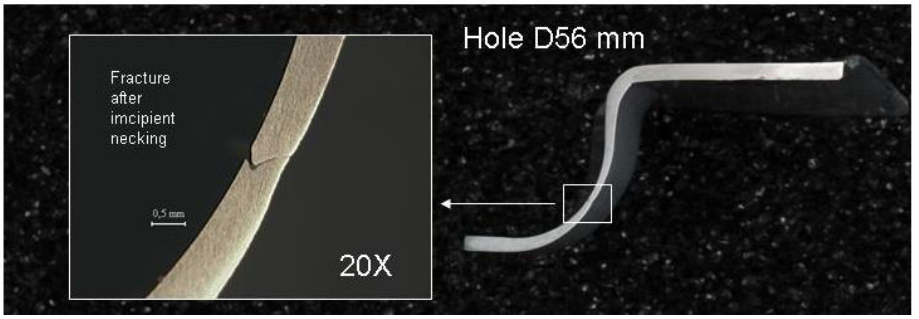

Fig. 8. Fractography of the failure zone for d_0 = 56 mm pre-cut hole specimen.

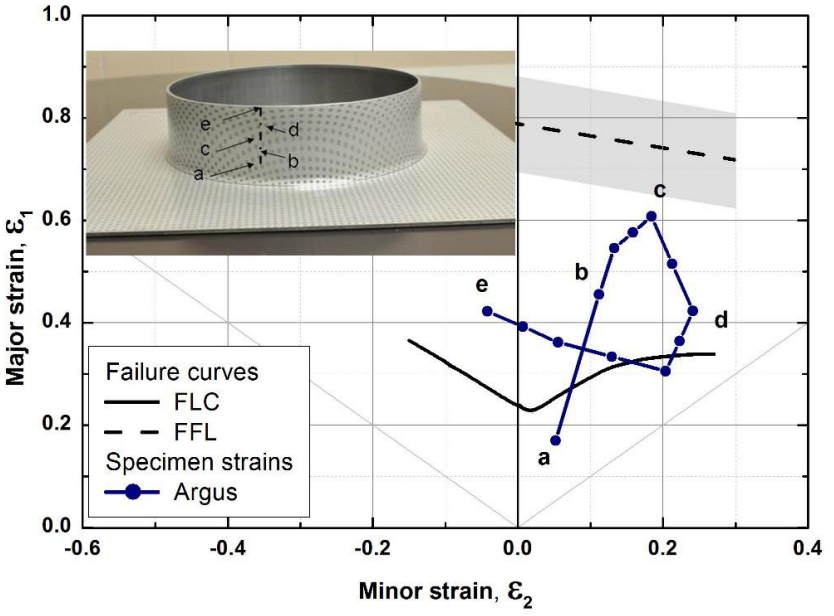

Fig. 9. Evolution of principal strains in the FLD for d_0 = 58 mm pre-cut hole specimen.

As mentioned before, a successful hole flanging operation was achieved for the specimen with a d_0 = 58 mm pre-cut hole. Fig. 9 shows the experimental results in the FLD for this specimen. Again, the *a-b-c-d-e* curve represents

the strains measured along a straight line over the sheet surface (see dot-dashed line in the up-left image in Fig. 9). As expected, in this case the measured strains are also well above the FLC but they do not reach the FFL. The shape of the strain distribution along the *a-b-c-d-e* line is similar as before, despite the fact that the flange is now well-formed. Compared with the previous case, the material in the zone *a-b-c* exhibits a higher tendency to a biaxial strain state, while the material near the edge (*d-e*) is deformed much more due the final stage of the flange formation. Note that near the hole edge, the material is mainly circumferentially stretched in the initial stages of the process and then, in the final stages, it is incrementally deformed by the tool under a combination of circumferential and radial stretching and bending.

4. Conclusions

Sheet metal flanged parts using a single-stage hole-flanging process by SPIF have been successfully obtained in 7075-O aluminum alloys of 1.6 mm thickness using a spherical 20 mm diameter forming tool. The limit forming ratio *LFR* obtained is above 1.62. This value agrees very well with similar studies reported in the literature.

The failure appears in the vertical wall of the part, instead of at the edge of the flange as usually observed in conventional hole-flanging operations. The mechanism of failure observed has been a postponed necking followed by ductile fracture. As a consequence the failure-control curve in the FLD is the FFL as usual in SPIF, and not the FLC as occurs in conventional sheet metal forming.

The understanding of the failure mechanisms and scope of application of the single-stage hole-flanging by SPIF encourages the use of this technology in industry in order to avoid costly equipment usually involved in the conventional hole-flanging process or to save time regarding the multistage strategies usually proposed in SPIF. The characterization of the influence of the key process parameters in the final shape of the formed part, such as tool geometry, tool path, tool rotation speed or hole geometry, opens an interesting area for future research.

Acknowledgements

The authors wish to thank the Spanish Government for its financial support through the research project DPI2012-32913.

References

[1] Z. Cui, L. Gao, Studies on hole-flanging process using multistage incremental forming, CIRP J. Manu. Sci. Tech. 2 (2010) 124–128.
[2] G. Centeno, M. B. Silva, V. A. M. Cristino, C. Vallellano, P. A. F. Martins, Hole-flanging by incremental sheet forming, Int. J. Mach. Tools Manu. 59 (2012) 46–54.
[3] V.A.M. Cristino, L. Montanari, M.B. Silva, A.G. Atkins, P.A.F. Martins, Fracture in hole-flanging produced by single point incremental forming. Int. J. Mech. Sci. 83 (2014) 146–154.
[4] V.A.M. Cristino, M. B. Silva, P.K.Wong, L.M. Tam, P.A.F. Martins, Hole-flanging of metals and polymers produced by single point incremental forming. Int. J. Mater. Prod. Technol. 50 (2015) 37–48.
[5] M.B. Silva, P.S. Nielsen, N. Bay, P.A.F. Martins, Failure mechanisms in single point incremental forming of metals, Int. J. Adv. Manuf. Technol. 56 (2011) 893–903.
[6] M. Bambach, H. Voswinckel, G. Hirt, A new process design for performing hole-flanging operations by incremental sheet forming, Procedia Engineering 81 (2014) 2305–2310.
[7] A.J. Martínez-Donaire, F.J. García-Lomas, C. Vallellano, New approaches to detect the onset of localised necking in sheets under through-thickness strain gradients, Mater. Des. 57 (2014) 135–145.
[8] M.B. Silva, M. Skjoedt, A.G. Atkins, N. Bay, P.A.F. Martins, Single-point incremental forming and formability-failure diagrams, J. Strain Anal. Eng. Des. 43 (2008) 15–35.
[9] Z. Liu, Y. Li, P. A. Meehan, Experimental investigation of mechanical Properties, formability and force measurement for AA7075-O aluminium alloy sheets formed by incremental forming, Int. J. Precis. Eng. Manuf. 14 (2013) 1891–1899.
[10] G. Centeno, I. Bagudanch, A.J. Martínez-Donaire, M.L. García-Romeu, C. Vallellano, Critical analysis of necking and fracture limit strains and forming forces in single-point incremental forming, Mater. Des. 63 (2014) 20–29.